

Epoxidation of cyclohexene with H₂O₂ over efficient water-tolerant heterogeneous catalysts composed of mono-substituted phosphotungstic acid on co-functionalized SBA-15

Manman Jin^{1,2} | Qingtao Niu² | Zhenmei Guo³ | Zhiguo Lv¹ 

¹State Key Laboratory Base for Eco-chemical Engineering, College of Chemical Engineering, Qingdao University of Science and Technology, No. 53 Zhengzhou Road, Qingdao 266042, China

²Department of Chemistry and Chemical Engineering, Jining University, Qufu, Shandong 273155, China

³College of Marine Science and Biological Engineering, Qingdao University of Science and Technology, No.53 Zhengzhou Road, Qingdao 266042, China

Correspondence

Zhiguo Lv, State Key Laboratory Base for Eco-chemical Engineering, College of Chemical Engineering, Qingdao University of Science and Technology, No. 53 Zhengzhou Road, Qingdao, 266042, China.
Email: lvzhiguo@qust.edu.cn

Funding information

National Natural Science Foundation of China, Grant/Award Number: NSFC21376128; Major Basic Research Projects of Shandong Provincial Natural Science Foundation, Grant/Award Number: ZR2017ZC0632

A series of Keggin-type heteropolyacid-based heterogeneous catalysts (Co-/Fe-/Cu-POM-octyl-NH₃-SBA-15) were synthesized via immobilized transition metal mono-substituted phosphotungstic acids (Co-/Fe-/Cu-POM) on octyl-amino-co-functionalized mesoporous silica SBA-15 (octyl-NH₂-SBA-15). Characterization results indicated that Co-/Fe-/Cu-POM units were highly dispersed in mesochannels of SBA-15, and both types of Brønsted and Lewis acid sites existed in Co-/Fe-/Cu-POM-octyl-NH₃-SBA-15 catalysts. Co-POM-octyl-NH₃-SBA-15 catalyst showed excellent catalytic performance in H₂O₂-mediated cyclohexene epoxidation with 83.8% of cyclohexene conversion, 92.8% of cyclohexene oxide selectivity, and 98/2 of epoxidation/allylic oxidation selectivity. The order of catalytic activity was Co-POM-octyl-NH₃-SBA-15 > Fe-POM-octyl-NH₃-SBA-15 > Cu-POM-octyl-NH₃-SBA-15. In order to obtain insights into the role of -octyl moieties during catalysis, an octyl-free catalyst (Co-POM-NH₃-SBA-15) was also synthesized. In comparison with Co-POM-NH₃-SBA-15, Co-POM-octyl-NH₃-SBA-15 showed enhanced catalytic properties (viz. activity and selectivity) in cyclohexene epoxidation. Strong chemical bonding between -NH₃⁺ anchored on the surface of SBA-15 and heteropolyanions resulted in excellent stability of Co-POM-octyl-NH₃-SBA-15 catalyst, and it could be reused six times without considerable loss of activity.

KEYWORDS

co-functionalized SBA-15, cyclohexene, epoxidation, heteropolyacid, mono-substituted

1 | INTRODUCTION

Cyclohexene oxide (viz. epoxide) synthesized via epoxidation of cyclohexene is indispensable for the fine-chemical industry.^[1] Nevertheless, two major side reactions, allylic oxidation and epoxide ring-opening, can considerably occur in epoxidation of cyclohexene, resulting in cyclohexene epoxidation to epoxide becoming difficult.^[2,3] Great efforts have been made in the development of new

active and selective catalysts for cyclohexene/olefins epoxidation to circumvent the above-mentioned side reactions and facilitate the formation of the desired product.^[4–9]

Polyoxometalates (POMs) have already been promising catalysts for plenty of oxidation reactions due to their acid property.^[10] Incorporation of transition metal into POM units (M-POMs) has aroused considerable interest as an efficient method to develop POM-derived catalysts.^[11–14] A primary disadvantage that impedes the actual

application of M-POMs in synthetic chemistry is that they are difficult to recycle. Heterogenization of M-POMs/POMs can offer materials that are much easier to separate, and may show improved selectivity and activities.^[15] This concept has been demonstrated in several systems,^[16] including V₂-POM/Support,^[17] GO/MNPs/PW,^[18] POM-poly^[19] and POM-ZrO₂.^[20] Despite interesting features of M-POMs-based heterogeneous catalysts, and recent progress in design and synthesis of these efficient catalysts, clean separation and recycling still present a considerable challenge.^[21,22] Concerning the diversity of M-POMs in composition, property and structure, there will be considerable scope for developing and designing more efficient heterogeneous M-POMs-based catalysts for olefins epoxidation reactions. It is interesting to note that the use of heterogeneous M-POMs-loaded materials that acted as catalysts in liquid (olefin)/liquid (H₂O₂)/solid (catalyst) triphase catalysis system is challenging, as mass transfer resistance exists between reactants. A crucial factor to improve catalytic activity is to control or regulate chemical features of the surface of solid supports, as the reaction rates of heterogeneous reactions should be determined via such surface processes as diffusion of reaction substrates and products, access of reactants to active center, as well as via microscopic environments around the catalysis center. It was worth mentioning that M-POMs could be chemically immobilized on some materials via forming positive charges on the support by surface modification to reduce the leaching of active species, and -NH₂ moieties could provide sites for the immobilization of charge matching components (viz. M-POMs). Further surface silylation with organic groups (-octyl, etc.) could improve the catalytic activity of as-synthesized catalyst via changing the surface properties to decrease mass transfer resistance between oil and water phases. To the best of our knowledge, there is no report for immobilization of M-POMs on -octyl and -NH₂ co-functionalized mesoporous silica SBA-15. In this case, heteropolyanions were

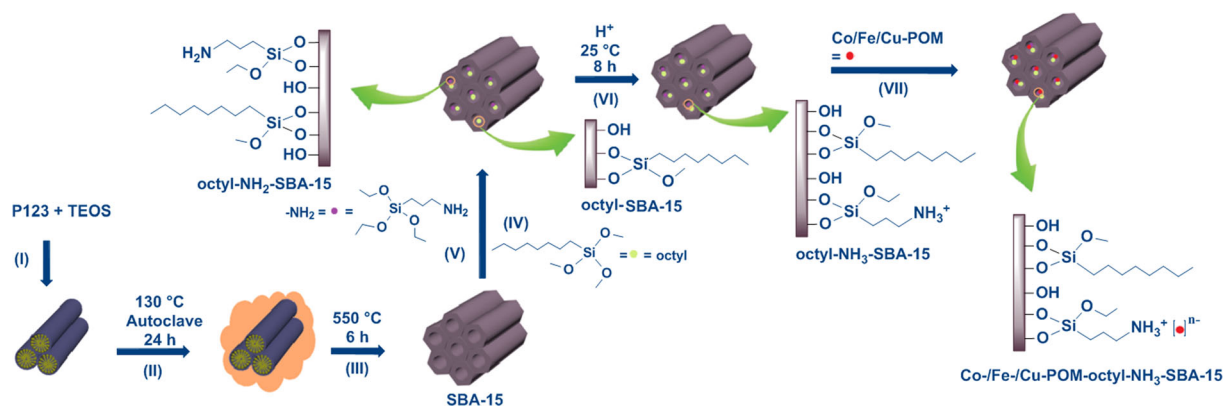
chemically bonded to -NH₃⁺ and surrounded with hydrophobic -octyl moieties in the mesochannels of SBA-15.

For the first time, we synthesized new and efficient Co-/Fe-/Cu-POM-based epoxidation catalysts using octyl-amino-co-functionalized mesoporous silica SBA-15 (octyl-NH₂-SBA-15) as a support. Si-OH groups that existed in SBA-15 structure were used as anchoring points for immobilization of -octyl and -NH₂ moieties via a post-synthetic strategy. In addition, -NH₃⁺ cations grafted on octyl-NH₂-SBA-15 were used for immobilization of Keggin-type Co-/Fe-/Cu-POM anions through electrostatic attraction. Co-/Fe-/Cu-POM-octyl-NH₃-SBA-15 catalysts with both Brønsted and Lewis acid sites showed excellent catalytic performance in cyclohexene epoxidation, and the order of catalytic activity was Co-POM-octyl-NH₃-SBA-15 > Fe-POM-octyl-NH₃-SBA-15 > Cu-POM-octyl-NH₃-SBA-15. Besides, Co-POM-octyl-NH₃-SBA-15 catalyst showed enhanced catalytic performance in cyclohexene epoxidation in comparison with immobilized Co-POM anions on octyl-free mesoporous SBA-15 (Co-POM-NH₃-SBA-15). The presence of -octyl moieties grafted in SBA-15 led to a more hydrophobic surface, which resulted in higher catalytic activity of synthesized materials.

2 | EXPERIMENTAL

2.1 | Catalysts preparation

The synthesis process of hybrid catalysts with nanostructure was illustrated in Scheme 1. Two different organic groups, -octyl and -NH₂, were successively grafted on Si-OH groups of SBA-15, respectively. [PW₁₁Co/Fe/CuO₄₀·yH₂O]ⁿ⁻ polyoxometalate anions were immobilized on acidulated amino groups (-NH₃⁺) via electrostatic binding, while hydrophobic regions around the polyanions were formed by anchored alkyl groups.



SCHEME 1 Schematic illustration of the synthesis concept of hybrid catalysts

2.1.1 | Synthesis of octyl-SBA-15

SBA-15 material was synthesized according to a previously reported procedure (Scheme 1).^[23] Octyl-SBA-15 (Scheme 1) was prepared by adding octyl-trimethoxysilane (-octyl, 1.0 mmol) to a suspension of SBA-15 (1.0 g) in anhydrous toluene (35 ml). The mixture was stirred and refluxed for 24 hr under N₂ protection. Subsequently, solid octyl-SBA-15 was collected by filtration, extracted with toluene using Soxhlet for 12 hr, and dried under vacuum. The synthetic process of NH₂-SBA-15 was similar to that of octyl-SBA-15, except that in this case 3-aminopropyltriethoxysilane was added instead of -octyl. Anal. found in NH₂-SBA-15: C, 8.55%; H, 2.02%; N, 1.63%.

2.1.2 | Preparation of octyl-NH₂-SBA-15

Typically, 3-aminopropyltriethoxysilane (1.0 mmol) was added to anhydrous toluene (35 ml) containing octyl-SBA-15 (1.0 g) while being stirred and refluxed for 24 hr under N₂ protection. Afterwards, the resulting octyl-NH₂-SBA-15 (Scheme 1) was filtered, extracted with toluene using Soxhlet for 12 hr, and dried under vacuum. Anal. found in octyl-NH₂-SBA-15: C, 10.94%; H, 2.56%; N, 1.57%.

2.1.3 | Synthesis of H_xPW₁₁Co/Fe/CuO₄₀·yH₂O

Co, Fe and Cu mono-substituted phosphotungstic acids were synthesized according to a modified procedure described by Tsigdinos *et al.*^[24] Typically, aqueous solution (20 ml) of Na₂HPO₄·12H₂O (0.01 mol) was mixed with aqueous solution (20 ml) of Co (NO₃)₂·6H₂O (0.01 mol). Concentrated sulfuric acid (about 1 ml) was added to the cooled mixture to obtain a bright red solution. Subsequently, aqueous solution (40 ml) of Na₂WO₄·2H₂O (0.11 mol) was added to the bright red solution and abundant flocculent precipitate immediately appeared. Afterwards, concentrated sulfuric acid (about 5 ml) was slowly added to the mixture with vigorous stirring to obtain a clear red solution. After the solution was cooled, heteropolyacid was extracted with 80 ml of ethyl ether and heteropoly etherate was located in the bottom layer. After separation and removing ether, the remaining red solid was dissolved in H₂O (50 ml) and crystallized to obtain the final H₇PW₁₁CoO₄₀·yH₂O (Co-POM). The above-mentioned synthetic process was repeated to prepare H₆PW₁₁FeO₄₀·yH₂O (Fe-POM) or H₇PW₁₁CuO₄₀·yH₂O (Cu-POM), except that in these cases Fe (NO₃)₃·9H₂O or Cu (NO₃)₂·3H₂O was added, respectively. Anal. found in Co-POM: P (1.07%), W (70.05%),

Co (2.05%); Fe-POM: P (1.07%), W (69.75%), Fe (2.13%); Cu-POM: P (1.08%), W (70.40%), Cu (2.23%). Anal. found in dehydrated Co-POM: H (0.24%), O (22.09%); dehydrated Fe-POM: H (0.23%), O (24.34%); dehydrated Cu-POM: H (0.24%), O (22.26%).

2.1.4 | Preparation of hybrid catalysts

Typically, octyl-NH₂-SBA-15 (0.5 g) or NH₂-SBA-15 (0.5 g) was mixed with trifluoromethanesulfonic acid (CF₃SO₃H, 2 mmol) while being stirred in CH₂Cl₂ (35 ml) for 8 hr. Subsequently, the solid was washed with ethyl alcohol and dried under vacuum to obtain the resultant material octyl-NH₃-SBA-15 or NH₃-SBA-15. Octyl-NH₃-SBA-15 (0.5 g) or NH₃-SBA-15 (0.5 g) was added to aqueous solution (30 ml) containing an appropriate amount of Co-/Fe-/or Cu-POM while being stirred and refluxed for 6 hr. The resulting solid was filtrated, washed with warm H₂O, and dried under vacuum to produce Co-/Fe-/or Cu-POM-octyl-NH₃-SBA-15 (Scheme 1) or Co-POM-NH₃-SBA-15 (*viz.* octyl-free catalyst). Anal. found in Co-POM-octyl-NH₃-SBA-15: C, 8.92%; H, 2.47%; N, 1.17%. Anal. found in Fe-POM-octyl-NH₃-SBA-15: C, 8.53%; H, 2.37%; N, 1.22%. Anal. found in Cu-POM-octyl-NH₃-SBA-15: C, 9.77%; H, 2.38%; N, 1.31%. Anal. found in Co-POM-NH₃-SBA-15: C, 5.27%; H, 1.92%; N, 1.21%.

2.2 | Characterization

N₂ adsorption isotherms were performed on ASAP 2020 V4.01 (V 4.01 H; Micromeritics) sorptometer at -196°C, and the samples were outgassed at 100°C for 8 hr before the measurement. X-ray diffraction (XRD) patterns were collected on a Rint 2000 vertical goniometer (Rigaku) using Cu K α radiation ($\lambda = 0.154$ nm) at 2°(2 θ)/min and operated at 30 mA and 40 kV. UV-Vis DRS spectra were gathered from 200 nm to 700 nm on a Cary 500 (8.01) spectrophotometer. Fourier transform-infrared (FT-IR) spectra were performed on a HGCS spectrometer from 4000 cm⁻¹ to 400 cm⁻¹ using material diluted with KBr. Thermal gravimetric analysis-difference thermogravimetry measurements were performed on a METTLER TGA/DSC1. The temperature was increased from 30°C to 700°C at a heating rate of 10°C/min under air atmosphere. Transmission electron microscopy (TEM) pictures were obtained by JEM-2100 electron microscope. The surface acidity of Co-/Fe-/Cu-POM-octyl-NH₃-SBA-15 was monitored from FT-IR spectra collected after pyridine adsorption. Typically, 100 mg of sample was degassed at 200°C under vacuum for 3 hr followed via absorbing pyridine. Then, excess pyridine was removed via heating

the sample at 120°C for 1 hr. Temperature-programmed desorption of adsorbed pyridine starting at 120°C was investigated by stepwise heating of the sample to characterize acid sites type and strength under vacuum. ³¹P-NMR spectrum of Co-POM was collected on an Aligent 600 MHz DD2 spectrometer.

2.3 | Catalytic tests

The catalytic performance was assessed via cyclohexene epoxidation with H₂O₂. In a typical run, cyclohexene (5 mmol), MeCN (5 ml) and catalyst (20 mg) were successively added to a round-bottomed flask while being stirred and heated at 65°C, and then 50 wt% H₂O₂ (18 mmol) was added drop by drop. The reaction was continued for 3 hr at 65°C with stirring. The details of cyclohexene epoxide acquisition and analysis were observed elsewhere.^[25]

3 | RESULTS AND DISCUSSION

3.1 | Catalytic characterization

The N₂ sorption experiment was carried out to investigate the mesoscopic quality and textural properties of synthesized materials. As shown in Figure 1(a) and (b), all sorption isotherms exhibited typical IV-type curves with clear

H1-type hysteresis loops, which was characteristic of a mesoporous structure with uniform pore size.^[26] This indicated that the ordered mesostructure was still maintained after introduction of organic moieties (viz. -octyl and -NH₂) and heteropolyanions into mesochannels of SBA-15. Compared with pure SBA-15, hysteresis loops of these hybrid materials shifted to lower relative pressure and became less vertical, illustrating that pore diameters (D_p) were decreased. Pore size distributions of SBA-15 and hybrid materials were depicted in Figure 1 (c) and (d). All samples exhibited monomodal distributions centered at 6.14–9.10 nm, suggesting the presence of uniform pore size and the existence of mesopores.

The texture parameters of these materials were summarized in Table 1. Compared with SBA-15, the specific surface area (S_{BET}), total pore volume (V_T) and D_p of silylated SBA-15 (i.e. octyl-SBA-15, NH₂-SBA-15 and octyl-NH₂-SBA-15) sharply decreased. As expected, Co-/Fe-/Cu-POM-octyl-NH₃-SBA-15 and Co-POM-NH₃-SBA-15 presented reduced S_{BET} , V_T and D_p compared with octyl-NH₂-SBA-15 and NH₂-SBA-15, respectively. This phenomenon confirmed the accommodation of Co-/Fe-/Cu-POM anions in the mesochannels of SBA-15. From inductively coupled plasma analysis, heteropolyanions contents in the solid catalysts were 0.108, 0.125, 0.141 and 0.117 mmol/g for Co-POM-octyl-NH₃-SBA-15, Fe-POM-octyl-NH₃-SBA-15, Cu-POM-octyl-NH₃-SBA-15 and Co-POM-NH₃-SBA-15, respectively.

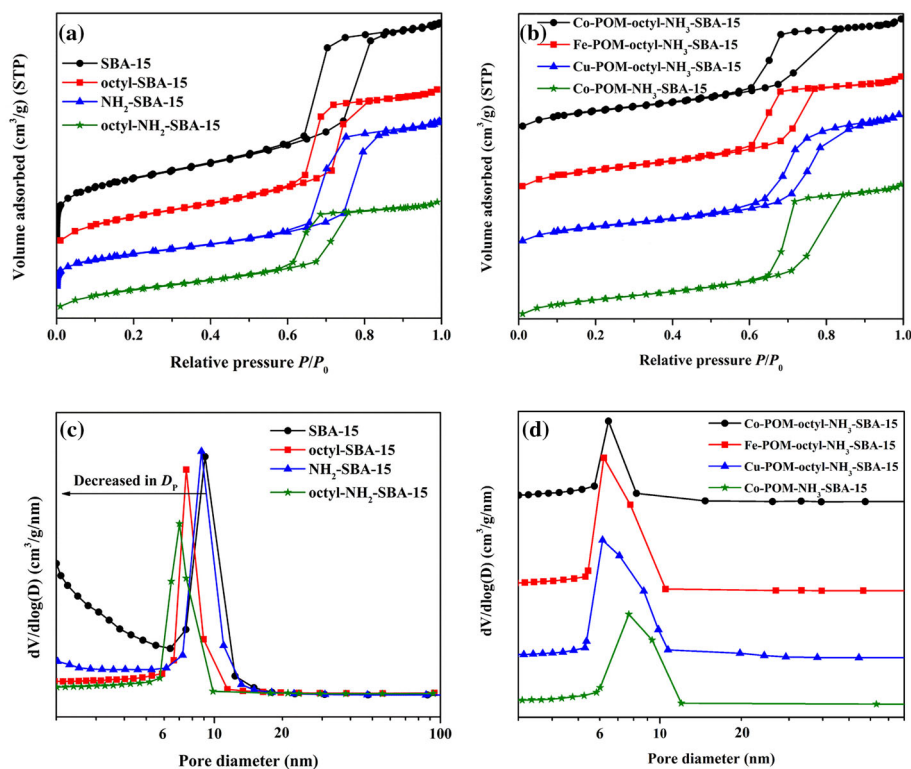


FIGURE 1 N₂ sorption isotherms (a and b) and pore size distributions (c and d) of synthesized materials

TABLE 1 Texture parameters of synthesized materials

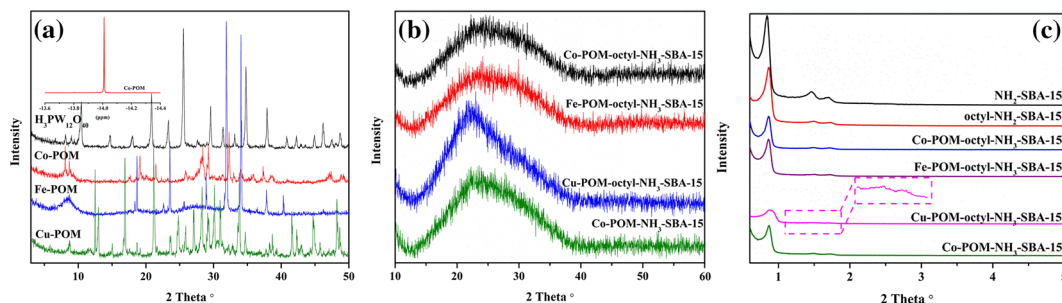
Samples	S_{BET} (m^2/g)	V_{T} (cm^3/g)	D_{p} (nm)	POM loading (mmol/g)
SBA-15	708	1.09	9.10	–
octyl-SBA-15	552	0.85	7.51	–
NH_2 -SBA-15	393	0.84	8.77	–
octyl- NH_2 -SBA-15	350	0.56	7.01	–
Co-POM-octyl- NH_3 -SBA-15	298	0.53	6.46	0.108
Fe-POM-octyl- NH_3 -SBA-15	324	0.51	6.20	0.125
Cu-POM-octyl- NH_3 -SBA-15	283	0.48	6.14	0.141
Co-POM- NH_3 -SBA-15	312	0.60	7.68	0.117

The wide-angle XRD patterns of Co-/Fe-/Cu-POM and $\text{H}_3\text{PW}_{12}\text{O}_{40}$ between 10° and 60° were displayed in Figure 2(a). $\text{H}_3\text{PW}_{12}\text{O}_{40}$ showed characteristic XRD peaks located at $2\theta = 8, 16\text{--}23, 25\text{--}30$ and $31\text{--}38^\circ$. In comparison with $\text{H}_3\text{PW}_{12}\text{O}_{40}$, partial substitution of W by Co/Fe/or Cu resulted in slight alteration in 2θ values of these characteristic peaks. For hybrid catalysts (Figure 2b), they all displayed a broad diffraction peak in $2\theta = 15\text{--}30^\circ$, which was the typical characterization of mesoporous silica. No characteristic peaks assigned to $\text{H}_3\text{PW}_{12}\text{O}_{40}$ were observed, which suggested homogeneous distribution of Co-/Fe-/Cu-POM units in the mesochannels of mesoporous SBA-15.

The small-angle XRD patterns of silylated SBA-15 and hybrid catalysts were exhibited in Figure 2(c). Silylated SBA-15 displayed an intense peak that corresponded to (100) reflection, and two relative weak peaks attributed to (110) and (200) reflections, which were indexed to highly ordered hexagonal lattice as reported.^[27] Immobilization of heteropolyanions on mesochannels of silylated SBA-15 resulted in slightly reduced intensities of these three reflection peaks with slight shifts to higher 2θ values compared with silylated SBA-15. Nevertheless, the mesostructure of SBA-15 still remained after silylation and heteropolyanions immobilization.

The FT-IR spectra of Co-/Fe-/Cu-POM and $\text{H}_3\text{PW}_{12}\text{O}_{40}$ were displayed in Figure 3(a). Typical IR bands ascribed to

phosphotungstic acid with Keggin type were detected in these spectra. Characteristic bands of $\text{H}_3\text{PW}_{12}\text{O}_{40}$ appeared at 1080 (P-O in central PO_4 tetrahedron stretching frequency), 973 (W=O in exterior WO_6 octahedron terminal bands), 889 (vibration of W-O_b-W bridge) and 810 cm^{-1} (band of W-O_c-W bridge), respectively. For Co-/Fe-/Cu-POM samples, corresponding bands (viz. 1080, 973, 889 and 810 cm^{-1}) slightly shifted, which was a description of distortion that resulted from partial replacement of W by Co/Fe/or Cu. The P-O band at 1080 cm^{-1} of $\text{H}_3\text{PW}_{12}\text{O}_{40}$ usually splits up into two bands for $(\text{PW}_{11})^{n-}$ (formed via substituting one W atom from $\text{H}_3\text{PW}_{12}\text{O}_{40}$),^[28] and the disappearance of the splitting of P-O absorption peaks in the FT-IR spectra of Co-/Fe-/Cu-POM was attributed to the introduction of Co, Fe or Cu into the quasi-octahedron vacancy of $(\text{PW}_{11})^{n-}$, the Co, Fe or Cu unit made up for the vacancy of $(\text{PW}_{11})^{n-}$ and restored the molecular symmetry.^[29] ^{31}P -MAS NMR spectroscopy was performed to further identify if there is any change in the environment around the phosphorus moiety. The ^{31}P -MAS NMR for $\text{H}_3\text{PW}_{12}\text{O}_{40}$ exhibited a chemical shift at -15.62 ppm,^[30] while that of Co-POM displayed a chemical shift at -14.01 ppm (Figure 2a, inset), indicating one W atom had been substituted by one transition metal atom.^[31] As seen in Figure 3(b), SBA-15 showed anti-symmetric and symmetric stretching vibration bands located at 1100 (ν_{as} Si-O-Si), 810 (ν_{s} Si-O-

**FIGURE 2** X-ray diffraction (XRD) patterns of synthesized materials

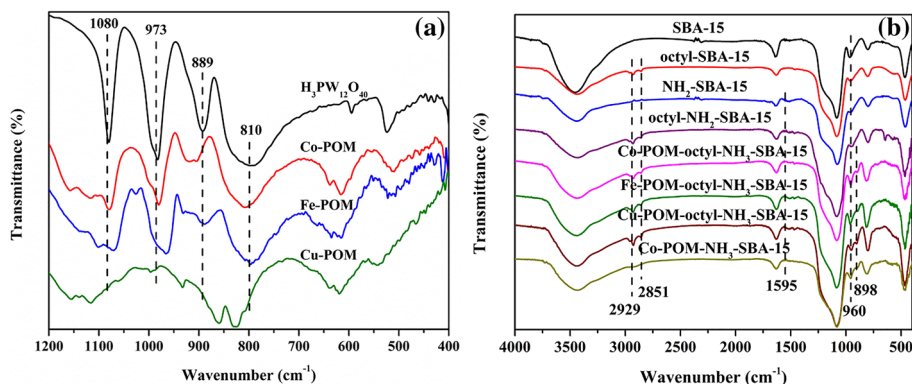


FIGURE 3 Fourier transform-infrared (FT-IR) spectra of $\text{H}_3\text{PW}_{12}\text{O}_{40}$ and synthesized materials

Si) and $460 (\delta \text{ Si-O-Si}) \text{ cm}^{-1}$. The bands at 3453, 1632 and 960 cm^{-1} were attributed to stretching vibrations of adsorbed H_2O molecules ($\delta \text{ H}_2\text{O}$) and Si-OH groups, respectively.^[32] For octyl-SBA-15, in addition to the bands originated from SBA-15, asymmetric and symmetric stretching of $-\text{CH}_2-$ at 2929 and 2851 cm^{-1} were observed, which suggested the alkyl groups were chemically grafted on SBA-15.^[33] New bands at 1595 cm^{-1} attributed to $-\text{N-H}$ bending vibration of $-\text{NH}_2$ were detected in octyl- NH_2 -SBA-15 and NH_2 -SBA-15, respectively,^[34] suggesting $-\text{NH}_2$ groups were successfully anchored in SBA-15. Stretching of $-\text{N-H}$ that appeared at 3380 and 3310 cm^{-1} was not detected, as it overlaid with broad band of surface Si-OH in the range of $3500\text{--}3000 \text{ cm}^{-1}$.^[35] Compared with NH_2 -SBA-15, the intensities of the other two bands of octyl- NH_2 -SBA-15 that corresponded to $-\text{CH}_2-$ stretching at 2935 and 2867 cm^{-1} increased. For Co-/Fe-/Cu-POM-octyl- NH_3 -SBA-15 and Co-POM- NH_3 -SBA-15 materials, an IR band that corresponded to vibration of W-O-W bridge was detected (898 cm^{-1}). The peak of W=O overlaid with the band of Si-OH in 960 cm^{-1} , and increased intensity of this band was clearly observed. The bands (i.e. 898 and 960 cm^{-1}) detected in FT-IR spectra of Co-/Fe-/Cu-POM-octyl- NH_3 -SBA-15 and Co-POM- NH_3 -SBA-15, regardless of the slight shift of bands positions, suggested the Keggin structure of phosphotungstic acid was well reserved.

The mesostructure and morphology of synthesized octyl- NH_2 -SBA-15 (Figure 4a and b) and Co-POM-octyl- NH_3 -SBA-15 (Figure 4c and d) were revealed via TEM analysis. As seen in Figure 4, highly uniform mesostructure and narrow pore distribution were clearly observed. This indicated that the mesostructure of SBA-15 remained intact after introduction of organic moieties and Co-/Fe-/Cu-POM units.

Figure 5 displayed UV-Vis spectra of initial SBA-15, Co-POM and hybrid Co-POM-octyl- NH_3 -SBA-15 catalyst. SBA-15 showed no peaks in 200–700 nm. Similar spectra were detected in Co-POM and Co-POM-octyl- NH_3 -SBA-

15. One peak at 265 nm corresponded to $\text{O} \rightarrow \text{W}$ charge transfer, and two broad bands centered at 340 and 550 nm attributed to the existence of Co (II) were detected.^[36] Particularly, the spectrum of Co-POM-octyl- NH_3 -SBA-15 differed from that reported about Co-POM datively linked to NH_2 -silica.^[37] Furthermore, no peaks and shoulders were detected between 628 nm and 640 nm, suggesting the dative bond between the amino group and cobalt was not formed.^[38] This manifested electrostatic binding between Co-POM and octyl- NH_3 -SBA-15.^[39]

The thermal behavior of representative samples (i.e. octyl- NH_2 -SBA-15 and Co-POM-octyl- NH_3 -SBA-15) was investigated via TG-DTA analyses (Figure 6). Co-POM-octyl- NH_3 -SBA-15 exhibited three obvious steps of mass loss between 30°C and 700°C . The first mass loss in $30\text{--}100^\circ\text{C}$ was ascribed to loss of adsorbed H_2O . The second mass loss occurred at 200°C due to removal of H_2O molecules per Keggin unit.^[40] The third mass loss in $300\text{--}530^\circ\text{C}$ was logical to ascribe to organic part decomposition in Co-POM-octyl- NH_3 -SBA-15, as octyl- NH_2 -SBA-15 exhibited similar major mass loss between 300°C and 530°C . The end of decomposition appeared at about $600\text{--}700^\circ\text{C}$, and constituent inorganic oxides were formed. Thermal analysis further confirmed Co-POM anions were successfully introduced to octyl- NH_2 -SBA-15 and Co-POM-octyl- NH_3 -SBA-15 catalyst was stable at the employed reaction temperature (65°C).

The pyridine adsorbed FT-IR analysis was carried out to evaluate the strength and types of acid sites of Co-/Fe-/Cu-POM-octyl- NH_3 -SBA-15 catalysts. Figure 7 exhibited pyridine FT-IR (Py-FT-IR) spectra of Co-POM-octyl- NH_3 -SBA-15 (Figure 7a), Fe-POM-octyl- NH_3 -SBA-15 (Figure 7b) and Cu-POM-octyl- NH_3 -SBA-15 (Figure 7c) catalysts recorded after adsorption of pyridine and subsequent evaluation at 120°C and 350°C . According to the literature,^[41] SBA-15 showed weak surface Lewis (L) acid sites after adsorption of pyridine at room temperature (RT), which vanished completely after outgassing at

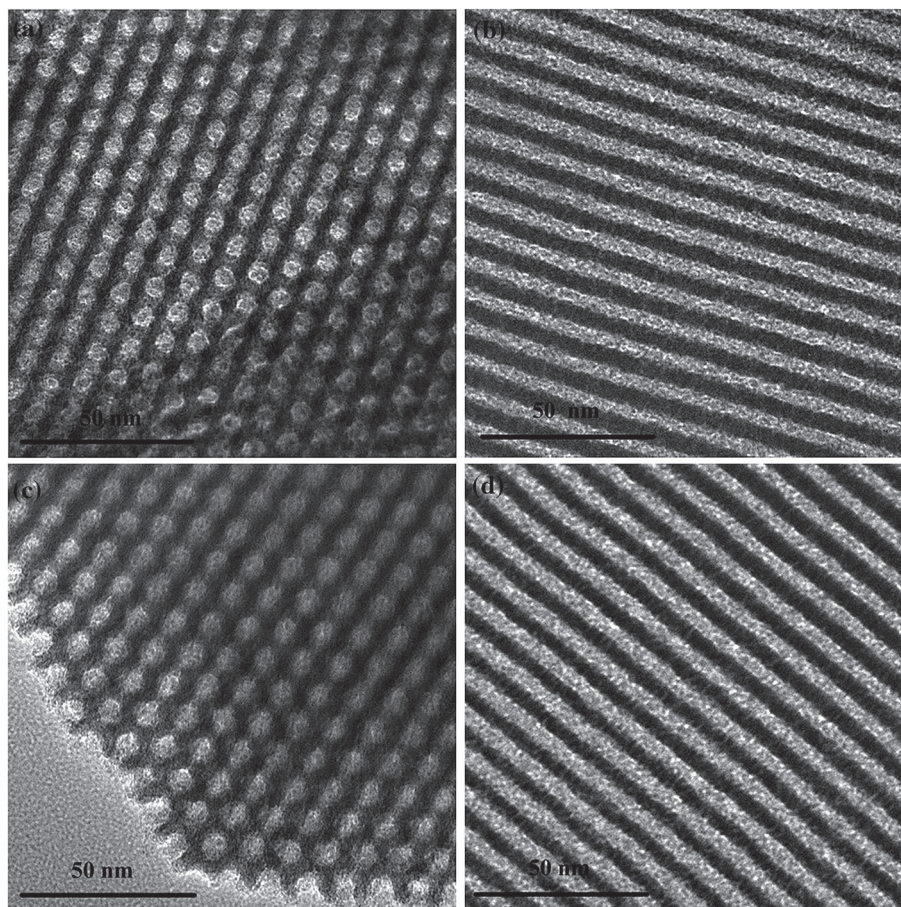


FIGURE 4 Transmission electron microscopy (TEM) images of octyl-NH₂-SBA-15 (a and b) and Co-POM-octyl-NH₃-SBA-15 (c and d). (a and c: along the [001] direction; b and d: along the [110] direction)

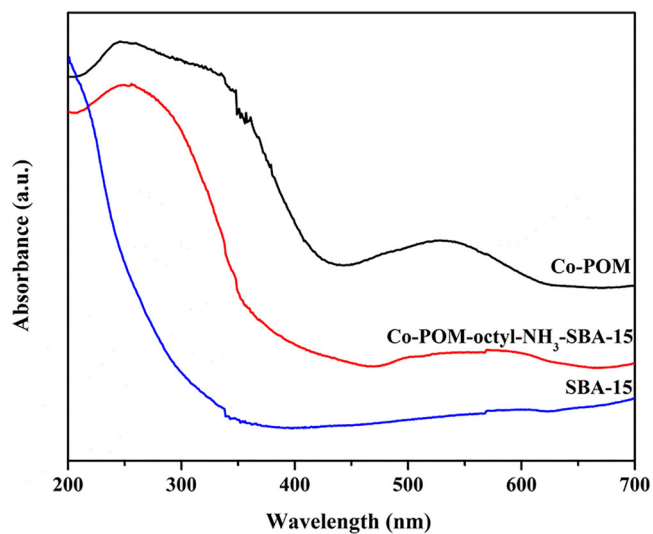


FIGURE 5 UV-Vis spectra of SBA-15, Co-POM and Co-POM-octyl-NH₃-SBA-15 catalyst

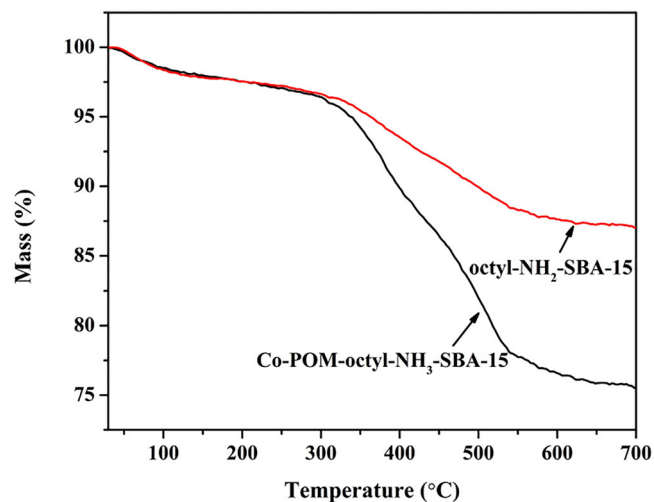


FIGURE 6 Thermogravimetric (TG)-differential thermal analysis (DTA) curves of octyl-NH₂-SBA-15 and Co-POM-octyl-NH₃-SBA-15 catalyst

200°C. Py-FT-IR spectra of Co-/Fe-/Cu-POM-octyl-NH₃-SBA-15 catalysts collected after adsorption of pyridine at RT showed bands at 1445 and 1595 cm⁻¹, assigned to pyridine coordinately bonded to weak surface L acid sites.^[42]

In addition to the bands located at 1445 and 1595 cm⁻¹, Co-/Fe-/Cu-POM-octyl-NH₃-SBA-15 catalysts also exhibited bands at 1488, 1545 and 1635 cm⁻¹ ascribed to protonated pyridine bonded to surface Brønsted (B) acid

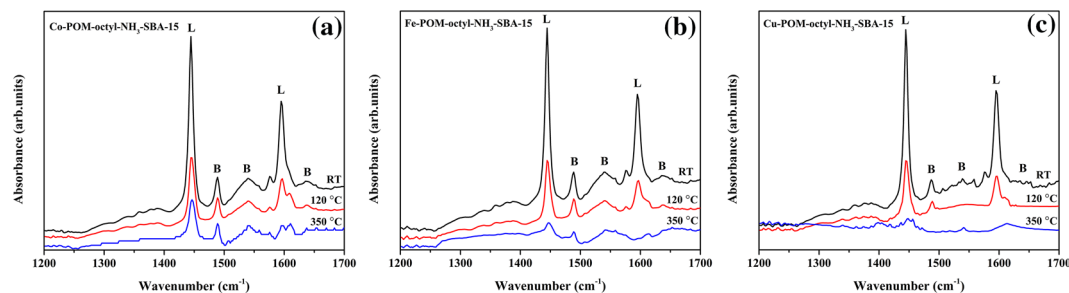


FIGURE 7 Pyridine adsorbed Fourier transform-infrared (FT-IR) spectra of Co-/Fe-/Cu-POM-octyl-NH₃-SBA-15 catalysts

sites, suggesting the existence of Co-/Fe-/Cu-POM anions led to the development of surface B acid sites. The intensities of these bands (i.e. 1445, 1488, 1545, 1595 and 1635 cm⁻¹) decreased after outgassing at rising temperature, but they were still recorded even after outgassing at 350°C, indicating that B and L acid sites in Co-/Fe-POM-octyl-NH₃-SBA-15 catalysts were rather strong. Nevertheless, for Cu-POM-octyl-NH₃-SBA-15 catalyst, all of these bands almost disappeared after outgassing at 350°C. As seen from Py-FT-IR spectra, the order of relative acid strength was Co-POM-octyl-NH₃-SBA-15 > Fe-POM-octyl-NH₃-SBA-15 > Cu-POM-octyl-NH₃-SBA-15. The relative amounts of B and L acid sites of Co-/Fe-/Cu-POM-octyl-NH₃-SBA-15 catalysts were summarized in Table 2. As seen from Table 2, the order of relative acid sites amounts was similar to that of acid strength. Based on Py-FT-IR analysis, it was concluded that both B and L acid sites existed in Co-/Fe-/Cu-POM-octyl-NH₃-SBA-15 catalysts. The strong B and L acid sites were essential to cyclohexene epoxidation.

3.2 | Catalytic epoxidation of cyclohexene

Catalytic activity of synthesized Co-/Fe-/Cu-POM-octyl-NH₃-SBA-15 and Co-POM-NH₃-SBA-15 catalysts was evaluated in cyclohexene epoxidation to epoxide using

H₂O₂ as oxidant. The results of catalytic performance of all obtained hybrid catalysts were listed in Table 3. Detectable products were cyclohexene oxide (epoxide), 1,2-cyclohexanediol (1,2-diol), 2-cyclohexene-1-ol (2-ol), 2-cyclohexene-1-one (2-one) and cyclohexenyl hydroperoxide (peroxide). Two different mechanisms, radical mechanism and direct epoxidation, existed in cyclohexene epoxidation. The existence of 2-ol originated from peroxide indicated partial reaction occurred via allylic oxidation, as depicted in Scheme 2; 2-one detected by gas chromatography (GC) essentially resulted from peroxide decomposition during GC analysis.^[43] Epoxide amount was far more than that obtained by radical mechanism, indicating direct epoxidation also took place. Cyclohexene conversion was as low as 6.9% (No. 1) in the absence of a catalyst. Co-POM-octyl-NH₃-SBA-15 (No. 2) exhibited high catalytic activity with cyclohexene conversion of 83.8%, epoxide selectivity of 92.8% and epoxidation/allylic selectivity of 98/2. When Fe-/Cu-POM-octyl-NH₃-SBA-15 acted as catalysts (No. 3–4), respectively, cyclohexene conversion of 72.5% and 58.5%, epoxide selectivity of 80.2% and 67.4%, and epoxidation/allylic selectivity of 91/9 and 87/13 were obtained. The order of catalytic activity was Co-POM-octyl-NH₃-SBA-15 > Fe-POM-octyl-NH₃-SBA-15 > Cu-POM-octyl-NH₃-SBA-15. This was explained by the different acidic strengths.^[44] The order of acidic strength was

TABLE 2 The relative acid sites amounts of Co-/Fe-/Cu-POM-octyl-NH₃-SBA-15 catalysts

Samples	Temperature (°C)	B amount (mmol/g)	L amount (mmol/g)	Total acidity (mmol/g)	B/L
Co-POM-octyl-NH ₃ -SBA-15	RT	190.34	493.40	683.74	0.39
	120	106.27	210.37	316.65	0.51
	350	79.14	155.65	234.79	0.51
Fe-POM-octyl-NH ₃ -SBA-15	RT	145.60	402.76	548.36	0.36
	120	91.27	149.99	241.26	0.61
	350	52.76	63.69	116.45	0.83
Cu-POM-octyl-NH ₃ -SBA-15	RT	58.81	352.82	411.63	0.17
	120	28.56	133.99	162.55	0.21
	350	12.05	37.03	49.08	0.33

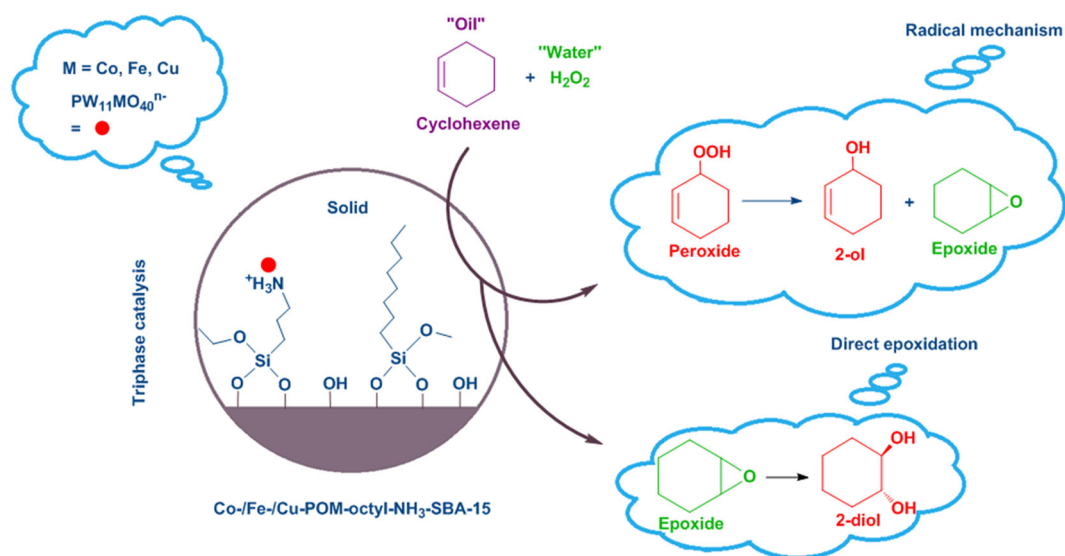
RT, room temperature.

TABLE 3 Catalytic performance of as-prepared catalysts in cyclohexene epoxidation with H₂O₂^a

No.	Catalysts	Cyclohexene Con. (%)	Selectivity (%)					Epoxide/ 1,2-diol	Epoxidation/ Allylic ox. ^b
			epoxide	1,2-diol	2-ol	2-one	others		
1	No	6.9	41.6	4.5	27.3	8.2	18.4	90/10	56/44
2	Co-POM-octyl-NH ₃ -SBA-15	83.8	92.8	3.7	0.8	1.6	1.1	96/4	98/2
3	Fe-POM-octyl-NH ₃ -SBA-15	72.5	80.2	7.3	3.2	5.6	3.7	92/8	91/9
4	Cu-POM-octyl-NH ₃ -SBA-15	58.5	67.4	6.1	5.8	5.4	15.3	92/8	87/13
5	Co-POM -NH ₃ -SBA-15	79.4	82.1	5.8	2.1	5.5	4.5	93/7	92/8

^aReaction conditions: m (catalyst) = 20 mg, n (cyclohexene) = 5 mmol, V (MeCN) = 5 ml, n(H₂O₂): n (cyclohexene) = 1.8:1, T = 65°C, t = 3 hr.

^b(Epoxide + diol)/(2-ol + 2-one).

**SCHEME 2** Mechanism of epoxidation of cyclohexene with H₂O₂^[2]

Co-POM-octyl-NH₃-SBA-15 > Fe-POM-octyl-NH₃-SBA-15 > Cu-POM-octyl-NH₃-SBA-15. Besides, Co-POM-octyl-NH₃-SBA-15 showed better catalytic performance than that of Co-POM-NH₃-SBA-15. As there were no distinct differences in their textural properties, therefore, this phenomenon indicated that the activity of Co-POM-octyl-NH₃-SBA-15 was obviously enhanced by a decrease of the number of Si-OH groups on the surface using octyl as the modified agent. Si-OH groups on the surface offered centers for adsorption of organic compounds like epoxide via hydrogen bonding. The diffusion to and away from the active sites in the mesochannels was impeded, which would decrease the overall catalytic activity of the catalyst.^[45] Converting partial Si-OH into Si-O-Si-octyl increased the hydrophobicity and the adsorption effect was reduced. The nanostructure of Co-POM-octyl-NH₃-SBA-15 provided a suitable environment for highly active epoxidation reaction, including a large specific interface area, active center on the hydrophobic interface, as well as the residual nanospaces in SBA-15 mesochannels,

thus an efficient diffusion of reactant molecules to active sites was realized. Higher epoxide selectivity (92.8%) and epoxidation/allylic oxidation selectivity (98/2) were obtained over Co-POM-octyl-NH₃-SBA-15 catalyst, hence, Co-POM-octyl-NH₃-SBA-15 was selected as the preferable catalyst to optimize the reaction conditions.

3.2.1 | Comparing catalytic efficiency of different heteropolyacid-based supported catalysts

Cyclohexene epoxidation to epoxide was selected as a probe reaction to compare catalytic efficiency of different heteropolyacid-based supported catalysts, and the comparison was in terms of reaction condition, reaction time and epoxide yield. As seen in Table 4, although other M-POM/POM-based supported materials catalyzed the reaction, they required higher reaction temperature and

TABLE 4 Comparison of catalytic efficiency of Co-POM-octyl-NH₃-SBA-15 with some different catalysts reported for cyclohexene epoxidation

No.	Catalyst	Reaction time (hr)	Reaction condition	Epoxide yield (%)	References
1	Co-POM-octyl-NH ₃ -SBA-15	3	MeCN/65 °C	77.8	This work
2	PW ₁₂ /AS-0.8-400	4	MeCN/80 °C	90	[46]
3	Ti-POM/MIL-101	6	MeCN/70 °C	< 8.58	[47]
4	PW ₁₂ /NH ₂ -SBA	3	MeCN/50 °C	7.5	[38]
5	Aerosil-Ti (O ⁱ Pr)	24	<i>t</i> -BuOH/80 °C	44.3	[48]
6	5% PW ₁₂ /MIL-101	3	MeCN/50 °C	67.2	[47]
7	PVMo-MCM-41	15	C ₂ H ₄ Cl ₂ /refluxed	19.8	[49]
8	PVMo-MCM-41-NH ₂	15	C ₂ H ₄ Cl ₂ /refluxed	9.45	[49]
9	PVMo-TiO ₂	12	MeCN/refluxed	70	[50]
10	PTA/Si-imid@Si-MNPs	6	C ₂ H ₄ Cl ₂ /70 °C	85.5	[51]

longer reaction time to reach comparable catalytic performance to Co-POM-octyl-NH₃-SBA-15 catalyst.

conversion and epoxide selectivity were 83% and 91%, respectively, which were similar to those of a fresh one.

3.3 | Reusability of Co-POM-octyl-NH₃-SBA-15 catalyst

The reusability of Co-POM-octyl-NH₃-SBA-15 catalyst in the cyclohexene epoxidation reaction was examined. After six consecutive reaction runs, consistent catalytic activity over Co-POM-octyl-NH₃-SBA-15 had been detected, establishing the fact that Co-POM-octyl-NH₃-SBA-15 could be recycled without any considerable loss of activity (Figure 8). The average values of cyclohexene

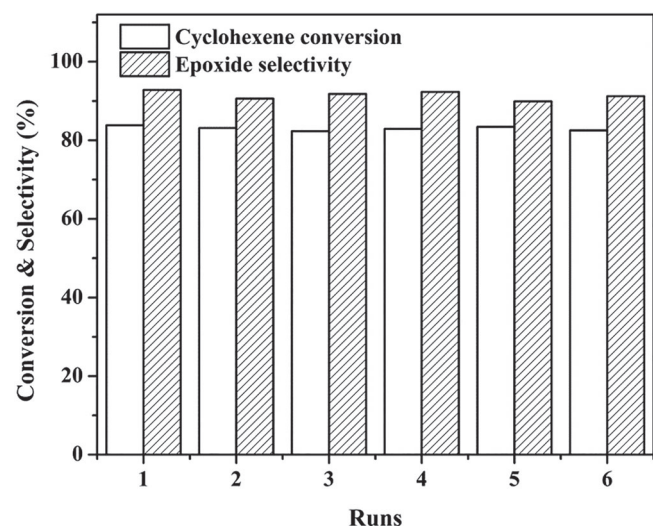


FIGURE 8 Reusability of Co-POM-octyl-NH₃-SBA-15 catalyst. Reaction conditions: *m* (Co-POM-octyl-NH₃-SBA-15) = 20 mg, *n* (cyclohexene) = 5 mmol, *n*(H₂O₂): *n* (cyclohexene) = 1.8:1, *V* (MeCN) = 5 ml, *T* = 65°C, *t* = 3 hr

3.3.1 | Hot filtration test

In order to check for any leaching of Co-POM anions into the solution during reaction, a hot-filtration test was carried out for the epoxidation reaction. Typically, cyclohexene (5 mmol) was allowed to react with H₂O₂ in MeCN medium with 20 mg of Co-POM-octyl-NH₃-SBA-15. The reaction was carried out at 65°C for 3 hr, and then the reaction mixture was immediately filtered under hot conditions. At this stage, epoxide yield was 77.8%. Subsequently, the reaction was continued at 65°C for a further 3 hr. Nevertheless, no increase of epoxide yield beyond 77.8% was detected. This result clearly reconfirmed the heterogeneous nature of Co-POM-octyl-NH₃-SBA-15. After six reaction runs, Co-POM content in Co-POM-octyl-NH₃-SBA-15 was marginally decreased to 0.101 mmol/g, which was 6.48% lower than that of the fresh one. These data revealed the fact that Co-POM units bonded to -NH₃ groups in the mesochannels of SBA-15 were purely heterogeneous in cyclohexene epoxidation.

Reused Co-POM-octyl-NH₃-SBA-15 catalyst (after the sixth run) was further characterized via UV-Vis and wide-angle XRD techniques to study if any further change occurred in Co-POM-octyl-NH₃-SBA-15 after reaction. Co-POM-octyl-NH₃-SBA-15 exhibited similar UV-Vis spectrum to the fresh one (Figure 9), suggesting Co-POM was still immobilized in the mesochannels of SBA-15 even after six reaction runs. Wide-angle XRD pattern of the recovered Co-POM-octyl-NH₃-SBA-15 (Figure 10) showed no characteristic peaks of Co-POM, indicating the Co-POM anions were still highly dispersed

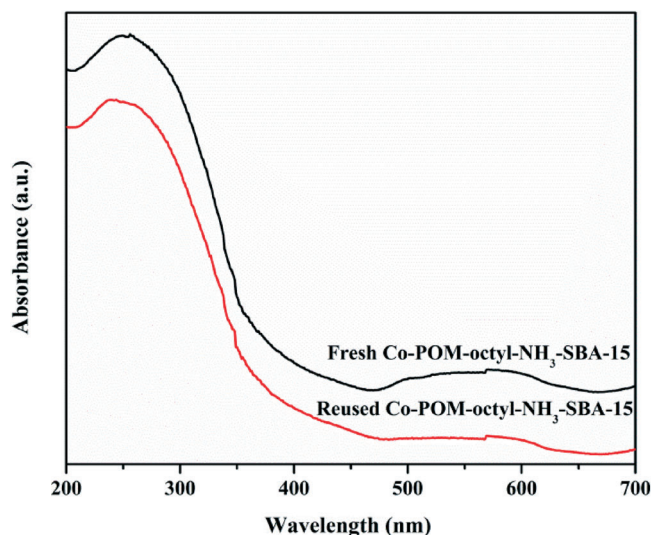


FIGURE 9 UV-Vis spectra of fresh and reused Co-POM-octyl-NH₃-SBA-15 catalyst

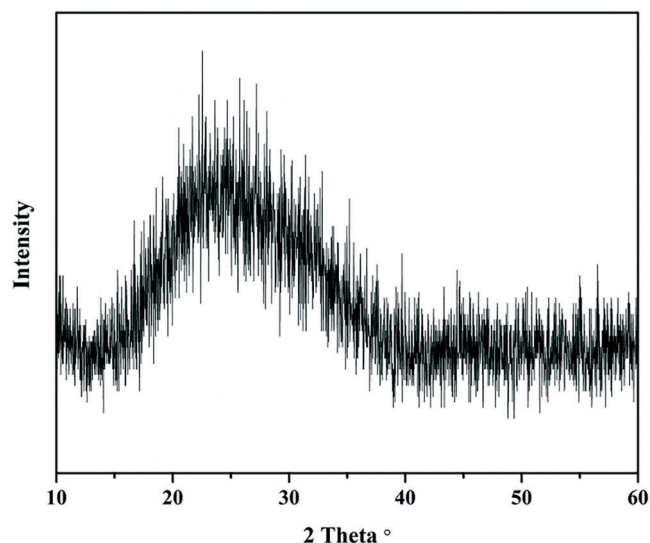


FIGURE 10 Wide-angle X-ray diffraction (XRD) pattern of recovered Co-POM-octyl-NH₃-SBA-15 catalyst

on SBA-15. The above results further confirmed that Co-POM-octyl-NH₃-SBA-15 had high stability and recyclability.

4 | CONCLUSIONS

Hybrid heterogeneous catalysts (Co-/Fe-/or Cu-POM-octyl-NH₃-SBA-15) were synthesized via grafting Co-/Fe-/or Cu mono-substituted phosphotungstic acids on octyl-amino-co-functionalized SBA-15. In H₂O₂-MeCN-mediated cyclohexene epoxidation reaction system, Co-POM-octyl-NH₃-SBA-15 showed excellent catalytic activity with cyclohexene conversion of 83.8%, epoxide

selectivity of 92.8% and epoxidation/allylic oxidation selectivity of 98/2. The order of catalytic activity was Co-POM-octyl-NH₃-SBA-15 > Fe-POM-octyl-NH₃-SBA-15 > Cu-POM-octyl-NH₃-SBA-15. Co-POM-octyl-NH₃-SBA-15 containing active species surrounded via hydrophobic alkyl groups in the mesochannels of SBA-15 showed better catalytic activity than that of octyl-free Co-POM-NH₃-SBA-15 catalyst. The more hydrophobic interface of SBA-15 might accelerate diffusion of reactants to catalysis center. Particularly, average values of 83% of cyclohexene conversion and 91% of epoxide selectivity were obtained over Co-POM-octyl-NH₃-SBA-15 for six reaction cycles. The superiority of the present study lies in achieving higher selectivity for the desired product epoxide, and suggests a prospective strategy for novel modified materials to develop an organic-inorganic cooperative function on the base of the nanostructure of mesoporous silica.

ACKNOWLEDGEMENTS

This work was supported by grants from Major Basic Research Projects of Shandong Provincial Natural Science Foundation (ZR2017ZC0632); National Natural Science Foundation of China (NSFC21376128).

ORCID

Zhiguo Lv  <https://orcid.org/0000-0001-6792-0088>

REFERENCES

- [1] Y. Ding, Q. Gao, G. Li, H. Zhang, J. Wang, L. Yan, J. Suo, *J. Mole. Catal. A Chem.* **2004**, *218*, 161.
- [2] J. M. Fraile, J. I. García, J. A. Mayoral, E. Vispe, *Appl. Catal. A* **2003**, *245*, 363.
- [3] J. M. Fraile, J. I. García, J. A. Mayoral, E. Vispe, *J. Catal.* **2000**, *189*, 40.
- [4] R. L. Brutchey, B. V. Mork, D. J. Sirbully, P. Yang, T. D. Tilley, *J. Mole. Catal. A Chem.* **2005**, *238*, 1.
- [5] D. C. Sherrington, S. Simpson, *J. Catal.* **2013**, *34*, 193.
- [6] M. E. Niño, S. A. Giraldo, E. A. Páezmozo, *J. Mole. Catal. A Chem.* **2001**, *175*, 139.
- [7] A. Zhang, L. Li, J. Li, Y. Zhang, S. Gao, *Cat. Com.* **2011**, *12*, 1183.
- [8] S. Akbarpour, A. Bezaatpour, E. Askarizadeh, M. Amiri, *Appl. Organomet. Chem.* **2017**, *31*, e3804.
- [9] V. Abbasi, H. H. Monfared, S. M. Hosseini, *Appl. Organomet. Chem.* **2016**, *31*, e3554.
- [10] H. Yu, S. Ru, G. Dai, Y. Zhai, H. Lin, S. Han, Y. Wei, *Angew. Chem. Int. Ed.* **2017**, *56*, 3867.
- [11] A. Marandi, S. Tangestaninejad, M. Moghadam, V. Mirkhani, A. Mechler, I. M. Baltork, F. Zadehahmadi, *Appl. Organomet. Chem.* **2018**, *32*, e4065.

- [12] E. Assady, B. Yadollahi, M. R. Farsani, M. Moghadam, *Appl. Organomet. Chem.* **2015**, *29*, 561.
- [13] V. Y. Evtushok, O. Y. Podyacheva, A. N. Suboch, N. V. Maksimchuk, O. A. Stonkus, L. S. Kibis, O. A. Kholdeeva, *Catal. Today* **2019**, *n/a*, n/a. <https://doi.org/10.1016/j.cattod.2019.03.060>
- [14] N. V. Maksimchuk, G. M. Maksimov, V. Y. Evtushok, I. D. Ivanchikova, Y. A. Chesalov, R. I. Maksimovskaya, O. A. Kholdeeva, A. Solé-Daura, J. M. Poblet, J. J. Carbó, *ACS Catal.* **2018**, *8*, 9722.
- [15] A. P. Wight, M. E. Davis, *Chem. Rev.* **2002**, *102*, 3589.
- [16] A. Patel, N. Narkhede, S. Singh, S. Pathan, *Catal. Rev.* **2016**, *58*, 337.
- [17] V. Y. Evtushok, A. N. Suboch, O. Y. Podyacheva, O. A. Stonkus, V. I. Zaikovskii, Y. A. Chesalov, L. S. Kibis, O. A. Kholdeeva, *ACS Catal.* **2018**, *8*, 1297.
- [18] M. M. Farahani, M. Modarres, *Appl. Organomet. Chem.* **2018**, *32*, e4142.
- [19] S. P. Maradur, C. Jo, D. H. Choi, K. Kim, R. Ryoo, *ChemCatChem* **2011**, *3*, 1435.
- [20] G. S. Armatas, G. Bilis, M. Louloudi, *J. Mater. Chem.* **2011**, *21*, 2997.
- [21] N. M. Okun, T. M. Anderson, C. L. Hill, *J. Am. Chem. Soc.* **2003**, *125*, 3194.
- [22] M. V. Vasylyev, R. Neumann, *J. Am. Chem. Soc.* **2004**, *126*, 884.
- [23] D. Zhao, J. Feng, Q. Huo, N. Melosh, G. H. Fredrickson, B. F. Chmelka, G. D. Stucky, *Science* **1998**, *279*, 548.
- [24] G. A. Tsigdinos, C. J. Hallada, *Inorg. Chem.* **1968**, *7*, 437.
- [25] T. Sreethawong, Y. Yamada, T. Kobayashi, S. Yoshikawa, *J. Mol. Catal. A Chem.* **2005**, *241*, 23.
- [26] S. Rohani, G. M. Ziarani, A. Badiei, A. Ziarati, M. Jafari, A. Shayesteh, *Appl. Organomet. Chem.* **2018**, *32*, e4397.
- [27] Q. Tang, Y. Wang, J. Zhang, R. Qiao, X. Xie, Y. Wang, Y. Yang, *Appl. Organomet. Chem.* **2016**, *30*, 435.
- [28] P. A. Shringarpure, A. Patel, *Synth. React. Inorg., Met.-Org., Nano-Met. Chem.* **2015**, *45*, 397.
- [29] X. Song, W. Zhu, K. Li, J. Wang, H. Niu, H. Gao, W. Gao, W. Zhang, J. Yu, M. Jia, *Catal. Today* **2016**, *259*, 59.
- [30] A. U. Patel, R. Sadasivan, *ChemistrySelect* **2018**, *3*, 11087.
- [31] L. Hua, Y. Qiao, Y. Yu, W. Zhu, T. Cao, Y. Shi, H. Li, B. Feng, Z. Hou, *New J. Chem.* **2011**, *35*, 1836.
- [32] S. Molaei, T. Tamoradi, M. Ghadermazi, A. G. Choghamarani, *Appl. Organomet. Chem.* **2019**, *33*, e4649.
- [33] H. Hoffmann, U. Mayer, A. Krischanitz, *Langmuir* **1995**, *11*, 1304.
- [34] E. Gianotti, V. Dellarocca, L. Marchese, G. Martra, S. Coluccia, T. Maschmeyer, *Phys. Chem. Chem. Phys.* **2002**, *4*, 6109.
- [35] S. W. Song, K. Hidajat, S. Kawi, *Langmuir* **2005**, *21*, 9568.
- [36] A. Patel, S. Pathan, *J. Coord. Chem.* **2012**, *65*, 3122.
- [37] B. J. S. Johnson, A. Stein, *Inorg. Chem.* **2001**, *40*, 801.
- [38] O. A. Kholdeeva, M. P. Vanina, M. N. Timofeeva, R. I. Maksimovskaya, T. A. Trubitsina, M. S. Melgunov, E. B. Burgina, J. M. Bialon, A. B. Jarzebski, C. L. Hill, *J. Catal.* **2004**, *226*, 363.
- [39] N. V. Maksimchuk, M. S. Melgunov, Y. A. Chesalov, J. M. Białoń, A. B. Jarzębski, O. A. Kholdeeva, *J. Catal.* **2007**, *246*, 241.
- [40] R. Tan, C. Liu, N. Feng, J. Xiao, W. Zheng, A. Zheng, D. Yin, *Micropor. Mesopor. Mater.* **2012**, *158*, 77.
- [41] X. Yang, W. Dai, R. Gao, K. Fan, *J. Catal.* **2007**, *249*, 278.
- [42] I. E. Wachs, *Catal. Today* **1996**, *27*, 437.
- [43] V. Lafond, P. H. Mutin, A. Vioux, *J. Mol. Catal. A Chem.* **2002**, *182–183*, 81.
- [44] P. Villabrille, G. Romanelli, L. Gassa, P. Vázquez, C. Cáceres, *Appl. Catal. A* **2007**, *324*, 69.
- [45] M. Jia, A. A. Seifert, W. R. Thiel, *Chem. Mater.* **2003**, *15*, 2174.
- [46] W. Cai, Y. Zhou, R. Bao, B. Yue, H. He, *Chin. J. Catal.* **2013**, *34*, 193.
- [47] N. V. Maksimchuk, K. A. Kovalenko, S. S. Arzumanov, Y. A. Chesalov, M. S. Melgunov, A. G. Stepanov, V. P. Fedin, O. A. Kholdeeva, *Inorg. Chem.* **2010**, *49*, 2920.
- [48] J. M. Fraile, J. I. García, J. A. Mayoral, E. Vispe, *Appl. Catal. A* **2003**, *245*, 363.
- [49] S. Tangestaninejad, V. Mirkhani, M. Moghadam, I. M. Baltork, E. Shams, H. Salavati, *Ultrason. Sonochem.* **2008**, *15*, 438.
- [50] S. Tangestaninejad, M. Moghadam, V. Mirkhani, I. M. Baltork, E. Shams, H. Salavati, *Cat. Com.* **2008**, *9*, 1001.
- [51] M. Kooti, M. Afshari, *Mater. Res. Bull.* **2012**, *47*, 3473.

How to cite this article: Jin M, Niu Q, Guo Z, Lv Z. Epoxidation of cyclohexene with H₂O₂ over efficient water-tolerant heterogeneous catalysts composed of mono-substituted phosphotungstic acid on co-functionalized SBA-15. *Appl Organometal Chem.* 2019;e5115. <https://doi.org/10.1002/aoc.5115>